Magnetohydroynamic Free Convection from a Disk Rotating in a Vertical Plane

William Thacker, Layne T. Watson
and S. Kishore Kumar

TR 88-52

MAGNETOHYDRODYNAMIC FREE CONVECTION FROM A DISK ROTATING IN A VERTICAL PLANE

William I. Thacker
Department of Computer Science
Winthrop College
Rock Hill, SC 29733

Layne T. Watson†
Department of Computer Science
Virginia Polytechnic Institute and State University
Blacksburg, VA 24061

S. Kishore Kumar‡
Department of Mathematics and Statistics
and
Department of Production Technology
Massey University
Palmerston North, New Zealand

Abstract. The non-axisymmetric motion (produced by a buoyancy induced cross flow) of a fluid in contact with a rotating disk and in the presence of a magnetic field normal to the disk is studied. Using modern quasi-Newton techniques, B-splines, and a Galerkin approximation to the fluid motion equations, numerical solutions are obtained for a wide range of magnetic field strengths and Prandtl numbers (ratio of kinematic viscosity to thermal conductivity). Results are presented both in tabular and graphical form in terms of two non-dimensional parameters. There is excellent agreement with previous work.

1. INTRODUCTION.

The axisymmetric character in rotating flows is destroyed when there are translational velocities imposed on a symmetric flow. Rott and Lewellen [1] studied a class of such flows. Their case belongs to the class of exact solutions of the Navier-Stokes equations discussed by Lin [2]. Recently, Chawla and Verma [3] obtained a solution to the free convective flow of a viscous incompressible fluid caused by a heated disk rotating in a vertical plane. Although this problem belongs to the class discussed in [2], the energy equation coupled with the momentum equation through buoyancy must be considered. The non-axisymmetric fluid motion is composed of the primary von Karman axisymmetric flow and a secondary buoyancy induced cross flow. Chawla and Verma [3] found transformations that uncouple the momentum and energy equations resulting in independent sets of equations that govern the

a) primary von Karman flow,

b) energy (dependent on the primary flow),

† Supported in part by AFOSR Grant 85-0250.
‡ Supported by University Grants Committee.

c) secondary cross flow (depends on both the primary von Karman flow and the energy).

The present study extends the scope of the work in [3] by imposing a magnetic field normal to the disk surface. Using the transformations in [3] for the flow variables, the governing momentum and energy equations uncouple resulting in

a) primary axisymmetric flow with an axial magnetic field (studied by Sparrow and Cess [4]),

b) an energy equation (dependent on the primary flow),

c) secondary cross flow (depends on both the primary flow and the energy).

2. FORMULATION OF THE PROBLEM.

Using a Cartesian coordinate system x, y, z, in a non-rotating reference frame, the x-axis is aligned with the negative direction of gravity g and the z-axis is horizontal. An infinite vertical disk is placed at $z = 0$ (i.e., in the x, y plane) in a viscous incompressible fluid. The disk rotates around the z axis with a constant angular velocity ω. There is a magnetic field of strength B_0 normal to the disk surface. The disk is at a constant temperature T_w and the fluid temperature far from the disk is T_∞. Using the analysis in [4], the governing magnetohydrodynamic (MHD) equations can be written as

$$u_x + v_y + w_z = 0, \tag{1}$$

$$uu_x + vu_y + wu_z = -\frac{1}{\rho}p_x + \nu\left(u_{xx} + u_{yy} + u_{zz}\right) + \beta g\left(T - T_\infty\right) - \sigma u B_0^2, \tag{2}$$

$$uv_x + vv_y + wv_z = -\frac{1}{\rho}p_y + \nu\left(v_{xx} + v_{yy} + v_{zz}\right) - \sigma B_0^2 v, \tag{3}$$

$$uw_x + vw_y + ww_z = -\frac{1}{\rho}p_z + \nu\left(w_{xx} + w_{yy} + w_{zz}\right), \tag{4}$$

$$uT_x + vT_y + wT_z = \kappa\left(T_{xx} + T_{yy} + T_{zz}\right), \tag{5}$$

where u, v and w are the velocity components in the x, y and z directions respectively. p is the pressure, T is the temperature, ρ is the fluid density, ν is the kinematic viscosity, β is the coefficient of thermal expansion, κ is the thermal conductivity of the fluid and σ is the electrical conductivity. The viscous dissipation is ignored as well as density variations except where necessary for deriving the buoyancy force.

The boundary conditions are

$$u = -y\omega, \qquad v = x\omega, \qquad w = 0, \qquad T = T_w, \qquad \text{at } z = 0, \tag{6}$$

$$u \to 0, \qquad v \to 0, \qquad T \to T_\infty, \qquad \text{as } z \to \infty. \tag{7}$$

Substituting the following similarity transformations:

$$u = \omega\left(-\frac{1}{2}xH'(\eta) - yG(\eta)\right) + \frac{g\beta\,(T_w - T_\infty)\,H_1(\eta)}{\omega}, \tag{8}$$

$$v = \omega\left(xG(\eta) - \frac{1}{2}yH'(\eta)\right) + \frac{g\beta\,(T_w - T_\infty)\,H_2(\eta)}{\omega}, \tag{9}$$

$$w = (\nu\omega)^{1/2}\,H(\eta), \tag{10}$$

$$p = -\rho\nu\omega P(\eta), \tag{11}$$

$$T = T_\infty + \Theta(\eta)\,(T_w - T_\infty)\,, \tag{12}$$

$$\eta = \left(\frac{\omega}{\nu}\right)^{1/2} z, \tag{13}$$

into equations (2)–(5) yields

$$H'''(\eta) - H(\eta)H''(\eta) + \frac{1}{2}(H'(\eta))^2 - 2G(\eta)^2 - mH'(\eta) = 0, \tag{14}$$

$$G''(\eta) - H(\eta)G'(\eta) + G(\eta)H'(\eta) - mG(\eta) = 0, \tag{15}$$

$$\Theta''(\eta) - \mathrm{Pr}\,H\Theta'(\eta) = 0, \tag{16}$$

$$H_1''(\eta) - H(\eta)H_1'(\eta) + \frac{1}{2}H_1(\eta)H'(\eta) + G(\eta)H_2(\eta) + \Theta(\eta) = 0, \tag{17}$$

$$H_2''(\eta) - H(\eta)H_2'(\eta) + \frac{1}{2}H_2(\eta)H'(\eta) - G(\eta)H_1(\eta) = 0, \tag{18}$$

where $\mathrm{Pr} = \nu/\kappa$ is the Prandtl number and $m = \sigma B_0^2/\rho\omega$ is the magnetic parameter. The boundary conditions (6) and (7) are also transformed and become

$$H(0) = 0, \quad H'(0) = 0, \quad G(0) = 1, \quad \Theta(0) = 1, \quad H_1(0) = 0, \quad H_2(0) = 0, \tag{19}$$

$$H'(\infty) = 0, \quad G(\infty) = 0, \quad \Theta(\infty) = 0, \quad H_1(\infty) = 0, \quad H_2(\infty) = 0. \tag{20}$$

In the absence of a magnetic field ($m = 0$), equations (14) and (15) were solved by von Karman [5], Cochran [6], Fettis [7], and Benton [8]. Sparrow and Cess [4] solved (14)–(16) to 4-digit accuracy for certain values of m and Pr values. Chawla and Verma [3] solved equations (14)–(18) for $m = 0$. The present investigation solves equations (14)–(18) numerically for a wide range of m and Pr values.

3. NUMERICAL METHOD.

Notice that equations (14) and (15) decouple from the rest of the system of equations (14)–(18). Once (14)–(15) are solved, equation (16) can be solved independent of equations (17) and (18). Then, after (14)–(16) are solved, the solutions to (17)–(18) can be determined.

In practice, the boundary conditions (20) are replaced by

$$H'(\tau) = G(\tau) = \Theta(\tau) = H_1(\tau) = H_2(\tau) = 0. \tag{21}$$

for some τ sufficiently large such that

$$|H(\eta) - H(\tau)| + |G(\eta)| + |\Theta(\eta)| + H_1(\eta)| + |H_2(\eta)| \approx 0 \text{ for } \tau \leq \eta < \infty. \tag{22}$$

Let S_n be the finite dimensional vector space with basis $\{B_{j,k,t}(x)\}_{j=1}^{n}$, where $B_{j,k,t}(x)$ is the jth B-spline of order k (degree $\leq k-1$) defined on the knot sequence $\mathbf{t} = (t_1, t_2, \cdots, t_{n+k})$. When there is no ambiguity, $B_{j,k,t}(x)$ is written as $B_j(x)$.

For this problem, the knot sequence $\mathbf{t}$ is based on the breakpoint sequence

$$\begin{aligned}
\Xi = (&.1, .2, .3, .4, .5, .6, .7, .8, .9, 1, 1.1, 1.2, 1.3, 1.4, 1.5, 1.6, 1.7, 1.8, 1.9,\\
&2, 2.1, 2.2, 2.3, 2.4, 2.5, 2.6, 2.7, 2.8, 2.9, 3, 3.2, 3.4, 3.6, 3.8, 4.0, 4.2, 4.4,\\
&4.6, 4.8, 5, 5.2, 5.4, 5.6, 5.8, 6, 6.2, 6.4, 6.6, 6.8, 7, 7.2, 7.4, 7.6, 7.8, 8, 8.25,\\
&8.5, 8.75, 9, 9.25, 9.5, 9.75, 10, 10.25, 10.5, 10.75, 11, 11.25, 11.5, 11.75, 12,\\
&12.25, 12.5, 12.75, 13, 13.25, 13.5, 13.75, 14, 14.5, 15, 15.5, 16, 16.5, 17, 17.5,\\
&18, 18.5, 19, 19.5, 20, 21, 22, 23, 24, 25, 26, 27, 28, 29, 30, 32, 34, 36, 38, 40, 43, 46,\\
&49, 53, 57, 61, 66, 71, 77, 83, 90, 98, 106, 114, 123, 133, 144, 156, 169, 183, 198, 214,\\
&231, 249, 268, 288, 309, 331, 354, 378, 403, 430, 460, 500, 550, 610, 690, 790, 900,\\
&1050, 1200, 1370, 1570, 1800, 2050, 2350, 2700, 3100, 3550, 4050, 4600, 5200, 5850,\\
&6550, 7300, 8100, 8950, 9850, 10850, 11900, 13000, 14150, 15350, 16600, 17900,\\
&19250, 20650, 22100, 23600, 25150, 26750, 28400, 30100, 31850, 33650, 35500, 37400,\\
&39350, 41350, 43400, 45500, 47650, 49850, 52100, 54400, 56750, 59150, 61600, 64100,\\
&66650, 69250, 71900, 74600, 77350, 80150, 83050, 86000, 89000, 92050, 95150, 98300,\\
&101500, 104750, 108050, 111400, 114800, 118250, 121750, 125300, 128900, 132550,\\
&136250, 140000, 143800, 147650, 151550, 155500, 159500, 163550, 167650, 171800,\\
&176000, 180250, 184550, 188900, 193300, 197750, 202250, 206800, 211400, 216050,\\
&220750, 225500, 230300, 235150, 240050, 245000, 250000, 255000, 260050, 265150,\\
&270300, 275500, 280800, 286200, 291700, 297300, 303000, 308800, 314700, 320700,\\
&326800, 333000, 339300, 345700, 352200, 358800, 365500, 372300, 379200, 386200,\\
&393300, 400500, 407800, 415200, 422700, 430300, 438000, 445800)
\end{aligned}$$

Following the convention used by deBoor [9] for the endpoints, set

$$t_1 = t_2 = \cdots = t_k \qquad \text{and} \qquad t_{n+1} = t_{n+2} = \cdots = t_{n+k}.$$

These repeated knots essentially mean the spline is free at the endpoints of the approximation interval $[t_k, t_{n+1}]$. Note that there is a distinction between knots and breakpoints [9]. All the knots in the approximation interval are simple, i.e., $t_i < t_{i+1}$. The functions $H(\eta)$, $G(\eta)$, $\Theta(\eta)$, $H_1(\eta)$, $H_2(\eta)$ have boundary layers (large derivatives) near $\eta = 0$, and asymptotically approach a constant as $\eta \to \infty$. The appropriate value for τ (unknown beforehand) is where solutions level off at their asymptotic value. Rather than dynamically adapting the knot sequence (which, as deBoor

[9] points out, is rarely cost effective), a reasonable strategy is to space the knots farther apart as η increases. Depending on the values of η and k, only an initial subsequence of the breakpoint sequence Ξ is used. For more details about B-splines see [9], and see [10] for a similar application.

The B-spline approximations used are

$$H(\eta) = \sum_{j=1}^{N+2} \alpha_j B_j(\eta), \tag{23}$$

$$G(\eta) = \sum_{j=1}^{N+2} \beta_j B_j(\eta), \tag{24}$$

$$\Theta(\eta) = \sum_{j=1}^{N+2} \gamma_j B_j(\eta), \tag{25}$$

$$H_1(\eta) = \sum_{j=1}^{N+2} \chi_j B_j(\eta), \tag{26}$$

$$H_2(\eta) = \sum_{j=1}^{N+2} \psi_j B_j(\eta). \tag{27}$$

The boundary conditions in equation (19) require

$$\alpha_1 = 0, \qquad \alpha_2 = 0, \qquad \beta_1 = 1, \qquad \gamma_1 = 1, \qquad \chi_1 = 0, \qquad \psi_1 = 0. \tag{28}$$

Similarly, the boundary conditions from equation (20) dictate

$$\alpha_{N+2} = \frac{-\alpha_{N+1} B'_{N+1}(\tau-)}{B'_{N+2}(\tau-)}, \qquad \beta_{N+2} = 0, \qquad \gamma_{N+2} = 0, \qquad \chi_{N+2} = 0, \qquad \psi_{N+2} = 0. \tag{29}$$

Using the standard Galerkin approximation, the nonlinear two-point boundary value problem given by equations (14)–(20) reduces to solving the nonlinear system of equations

$$\begin{aligned}
\langle H''' - HH'' + (H')^2/2 - 2G^2 - mH', B_i\rangle &= 0, \qquad i = 3, \ldots, N+1,\\
\langle G'' - HG' + GH' - mG, B_i\rangle &= 0, \qquad i = 2, \ldots, N+1,\\
\langle \Theta'' - \Pr H\Theta', B_i\rangle &= 0, \qquad i = 2, \ldots, N+1,\\
\langle H_1'' - HH_1' + H_1H'/2 + GH_2 + \Theta, B_i\rangle &= 0, \qquad i = 2, \ldots, N+1,\\
\langle H_2'' - HH_2' + H_2H'/2 - GH_1, B_i\rangle &= 0, \qquad i = 2, \ldots, N+1,
\end{aligned} \tag{30}$$

where

$$\langle u, v\rangle = \int_0^\tau u(\eta)v(\eta)\,d\eta.$$

Let

$$\begin{aligned}
Y_1 &= (\alpha_3, \alpha_4, \ldots, \alpha_{N+1}, \beta_2, \beta_3, \ldots, \beta_{N+1})^t,\\
Y_2 &= (\gamma_2, \gamma_3, \ldots, \gamma_{N+1})^t,\\
Y_3 &= (\chi_2, \chi_3, \ldots, \chi_{N+1}, \psi_2, \psi_3, \ldots, \psi_{N+1})^t,
\end{aligned}$$

and let $F_1(Y_1) = 0$ be given by the first $p_1 = 2N - 1 = 2n - 5$ equations of (30), $F_2(Y_2) = 0$ by the next $p_2 = N = n - 2$ equations, and $F_3(Y_3) = 0$ by the last $p_3 = 2N = 2n - 4$ equations. As mentioned earlier, the equations (30) decouple; first $F_1(Y_1) = 0$ is solved, then $F_2(Y_2) = 0$, and finally $F_3(Y_3) = 0$.

Two methods were used to solve for the Y_i, a quasi-Newton method and a globally convergent homotopy method. The quasi-Newton method used was subroutine **HYBRD** from the **MINPACK** subroutine package developed by Argonne National Laboratory [11]. The other method used was subroutine **FIXPNF**, a globally convergent homotopy method in the subroutine package **HOMPACK** developed by Watson et al. [12] which does not fail by converging to nonzero local minima of $F_i(Y_i)^t F_i(Y_i)$ as **MINPACK** does at times. However, the homotopy method may require considerably more computation time. Details about **HOMPACK** and some of its applications can be found in [12]–[15].

This Galerkin formulation is more numerically stable than previously used shooting techniques [16], [17], [18] and [19] for similar MHD problems. However, with starting values not "close enough" to the solution, **HYBRD** still failed at times. The strategy employed in this study was to solve one problem using the **HOMPACK** subroutine package [12]. After a solution to one problem was found, it was used as the starting point for a nearby problem. This starting point was usually sufficiently close to the solution of the problem for **HYBRD** to converge. The parameter ranges were systematically explored using **FIXPNF** whenever **HYBRD** failed.

Another aspect of the problem was to determine an appropriate value of τ. The value of τ is inferred from N, k, and the breakpoint sequence Ξ. The method employed in this study was to try one value for N and examine $H''(\tau)$, $G'(\tau)$, $\Theta'(\tau)$, $H_1'(\tau)$, and $H_2'(\tau)$. If these values were close to zero, the value of N was accepted. Otherwise, the value of N was increased. Increasing N drastically increased the amount of computer time needed to solve the problem, and some cases were too expensive to solve.

The integrals in (30) are evaluated by a 10-point Gaussian quadrature over each interval and are essentially exact. For all the cases a k of 6 (order of the B-spline) was used. This produces results with an accuracy of $O(h^6) = O((.1)^6) = O(10^{-6})$.

The B-spline approximations and their derivatives were evaluated using the subroutine package contained in [9]. It is quite easy to find the maximum and minimum values of the functions H_1 and H_2 by finding the roots of their derivatives.

4. DISCUSSION.

The buoyancy induced cross flow depends on two parameters, m and Pr. The effect of these parameters is presented graphically in Figures 1 and 2. $m = 0$ is the case of a rotating disk in the absence of a magnetic field, studied in [3].

Figures 1a and 1b show the effects of m on buoyancy induced cross flow (H_1 and H_2). These profiles show that their boundary layers are much thicker than the primary Von Karman boundary layer ($m = 0$). As m increases, the thickness of the superimposed free convection boundary layer increases. Figures 2a and 2b show the effect of Pr on H_1 and H_2 for $m = 1.0$. These show a decrease in the boundary layer thickness as Pr increases.

The effects of m and Pr on the coefficient of heat transfer $\Theta'(0)$ and the coefficients of skin friction $H_1'(0)$ and $H_2'(0)$ corresponding to the cross flow are shown in Tables 1, 2 and 3 respectively. For $m = 0$, there is good agreement between the current technique and previous results [3]. From Table 1, we can conclude that the coefficient of heat transfer decreases as m increases and increases as Pr increases. The shear stresses ($H_1'(0)$ – Table 2 and $H_2'(0)$ – Table 3) increase as m increases and decreases as Pr increases.

On a finite disk of radius R, the resulting force is given by

$$\rho g \beta \pi R^2 (T_w - T_\infty)(\nu/\omega)^{1/2}[(H_1'(0))^2 + (H_2'(0))^2] \tag{31}$$

From Tables 2 and 3 and expression (31), we see that the resultant force increases as m increases and decreases as Pr increases.

Table 4 gives the maximum and minimum values and where they occur for H_1 for various m and Pr values. As m increases, the maximum value increases and the point where this maximum occurs is increased. An opposite effect is seen by increasing Pr. Table 5 shows similar effects for H_2.

Pr\m	0.0*	0.0	0.5	1.0	1.5	2.0	3.0	4.0
5.00	0.6920	0.8533	0.6948	0.5589	0.4498	0.3644	0.2478	0.1780
4.00	n/a	0.7753	0.6235	0.4929	0.3893	0.3101	0.2060	0.1460
3.00	0.6826	0.6826	0.5389	0.4153	0.3195	0.2491	0.1609	0.1124
2.50	0.6280	0.6280	0.4892	0.3703	0.2801	0.2155	0.1370	0.0949
2.00	0.5620	0.5653	0.4324	0.3197	0.2368	0.1794	0.1121	0.0770
1.80	0.5370	0.5371	0.4071	0.2975	0.2182	0.1642	0.1018	0.0696
1.60	0.5080	0.5068	0.3798	0.2739	0.1988	0.1485	0.0913	0.0623
1.40	0.4734	0.4737	0.3504	0.2488	0.1784	0.1322	0.0806	0.0548
1.20	0.4371	0.4371	0.3182	0.2220	0.1571	0.1154	0.0698	0.0472
1.00	n/a	0.3962	0.2827	0.1930	0.1346	0.0980	0.0587	0.0396
0.90	0.3737	0.3737	0.2633	0.1777	0.1229	0.0890	0.0531	0.0357
0.80	0.3495	0.3494	0.2428	0.1617	0.1108	0.0799	0.0474	0.0319
0.70	0.3231	0.3231	0.2209	0.1449	0.0984	0.0706	0.0417	0.0280
0.60	0.2943	0.2943	0.1974	0.1274	0.0857	0.0611	0.0359	†
0.50	0.2623	0.2623	0.1720	0.1090	0.0725	0.0515	0.0301	†
0.40	0.2263	0.2263	0.1444	0.0896	0.0590	0.0416	0.0242	†
0.30	0.1849	0.1849	0.1141	0.0691	0.0450	0.0315	0.0182	†
0.20	0.1361	0.1361	0.0805	0.0475	0.0305	0.0212	†	†
0.10	0.0766	0.0766	0.0428	0.0245	†	†	†	†
0.04	0.0333	0.0333	0.0178	†	†	†	†	†
0.01	0.0087	0.0087	0.0046	†	†	†	†	†

Table 1. Effect of Pr and m on $-\Theta'(0)$ (*-column from Chawla and Verma [3]). n/a : not available, †: asymptotic range beyond last breakpoint.

Pr\m	0.0*	0.0	0.5	1.0	1.5	2.0	3.0	4.0
5.00	0.5173	0.5161	0.6599	0.8889	1.2333	1.7045	2.9831	4.6079
4.00	n/a	0.5561	0.7231	1.0031	1.4395	2.0428	3.6717	5.7236
3.00	0.6132	0.6131	0.8180	1.1859	1.7815	2.6098	4.8257	7.5886
2.50	0.6530	0.6530	0.8878	1.3283	2.0550	3.0658	5.7524	9.0834
2.00	0.7066	0.7064	0.9863	1.5388	2.4661	3.7530	7.1460	11.3282
1.80	0.7338	0.7337	1.0387	1.6548	2.6950	4.1360	7.9214	12.5761
1.60	0.7660	0.7659	1.1026	1.7993	2.9816	4.6156	8.8916	14.1366
1.40	0.8051	0.8050	1.1827	1.9845	3.3509	5.2334	10.1398	16.1437
1.20	0.8540	0.8539	1.2869	2.2310	3.8444	6.0588	11.8054	18.8205
1.00	n/a	0.9178	1.4295	2.5759	4.5370	7.2163	14.1388	22.5691
0.90	0.9583	0.9583	1.5230	2.8058	4.9995	7.9890	15.6951	25.0686
0.80	1.0071	1.0070	1.6388	3.0933	5.5783	8.9555	17.6410	28.1933
0.70	1.0674	1.0673	1.7864	3.4632	6.3235	10.1992	20.1435	32.2111
0.60	1.1448	1.1446	1.9815	3.9568	7.3182	11.8587	23.4808	†
0.50	1.2491	1.2489	2.2529	4.6485	8.7123	14.1833	28.1540	†
0.40	1.3998	1.3995	2.6576	5.6873	10.8056	17.6722	35.1653	†
0.30	1.6423	1.6419	3.3293	7.4207	14.2976	23.4899	46.8526	†
0.20	2.1130	2.1118	4.6693	10.8915	21.2870	35.1286	†	†
0.10	3.4921	3.4879	8.6842	21.3146	†	†	†	†
0.04	7.5993	7.5713	20.7269	†	†	†	†	†
0.01	28.4073	27.9392	80.9462	†	†	†	†	†

Table 2. Effect of Pr and m on $H_1'(0)$ (*-column from Chawla and Verma [3]). †: asymptotic range beyond last breakpoint.

Pr\m	0.0*	0.0	0.5	1.0	1.5	2.0	3.0	4.0
5.00	0.0923	0.0916	0.1544	0.2533	0.3793	0.5162	0.7775	0.9991
4.00	n/a	0.1059	0.1831	0.3102	0.4754	0.6541	0.9879	1.2653
3.00	0.0279	0.1278	0.2297	0.4065	0.6402	0.8895	1.3428	1.7113
2.50	0.1444	0.1443	0.2664	0.4851	0.7750	1.0811	1.6288	2.0693
2.00	0.1678	0.1678	0.3212	0.6052	0.9811	1.3720	2.0598	2.6074
1.80	0.1804	0.1803	0.3516	0.6729	1.0970	1.5349	2.3000	2.9067
1.60	0.1957	0.1957	0.3897	0.7583	1.2430	1.7395	2.6006	3.2811
1.40	0.2151	0.2151	0.4389	0.8694	1.4322	2.0037	2.9878	3.7626
1.20	0.2403	0.2403	0.5049	1.0193	1.6864	2.3575	3.5047	4.4051
1.00	0.2976	0.2748	0.5981	1.2318	2.0449	2.8548	4.2292	5.3049
0.90	0.3258	0.2976	0.6607	1.3748	2.2851	3.1871	4.7126	5.9049
0.80	0.3538	0.3258	0.7396	1.5547	2.5865	3.6033	5.3171	6.6551
0.70	0.3618	0.3617	0.8418	1.7875	2.9751	4.1392	6.0947	7.6198
0.60	0.4095	0.4095	0.9793	2.0998	3.4949	4.8547	7.1319	†
0.50	0.4762	0.4761	1.1737	2.5398	4.2247	5.8577	8.5845	†
0.40	0.5763	0.5762	1.4683	3.2036	5.3220	7.3640	10.7641	†
0.30	0.7440	0.7437	1.9648	4.3160	7.1549	9.8767	14.3977	†
0.20	1.0827	1.0820	2.9687	6.5508	10.8270	14.9055	†	†
0.10	2.1135	2.1109	6.0096	13.2787	†	†	†	†
0.04	5.2477	5.2299	15.1784	†	†	†	†	†
0.01	21.1869	20.8860	61.0891	†	†	†	†	†

Table 3. Effect of Pr and m on $-H_2'(0)$ (*-column from Chawla and Verma [3]). †: asymptotic range beyond last breakpoint.

m	0.0		0.5		1.0		1.5	
Pr	$\bar{\eta}$	$H_1(\bar{\eta})$	$\bar{\eta}$	$H_1(\bar{\eta})$	$\bar{\eta}$	$H_1(\bar{\eta})$	$\bar{\eta}$	$H_1(\bar{\eta})$
5.00	0.817	0.171	1.139	0.293	1.785	0.576	2.762	1.206
4.00	0.877	0.199	1.260	0.354	2.048	0.750	3.171	1.669
3.00	0.966	0.242	1.452	0.460	2.449	1.081	3.762	2.580
2.50	1.030	0.275	1.599	0.549	2.738	1.382	4.175	3.421
2.00	1.120	0.323	1.812	0.691	3.123	1.892	4.720	4.848
1.80	1.167	0.349	1.926	0.775	3.316	2.204	4.994	5.717
1.60	1.224	0.382	2.065	0.886	3.539	2.619	5.313	6.871
1.40	1.295	0.424	2.235	1.036	3.802	3.192	5.690	8.456
1.20	1.387	0.481	2.448	1.252	4.117	4.017	6.147	10.725
1.00	1.513	0.562	2.719	1.581	4.506	5.277	6.719	14.160
0.90	1.595	0.618	2.884	1.818	4.738	6.175	7.064	16.593
0.80	1.695	0.690	3.074	2.131	5.005	7.356	7.464	19.774
0.70	1.821	0.786	3.296	2.559	5.316	8.958	7.933	24.063
0.60	1.983	0.921	3.558	3.171	5.687	11.217	8.498	30.079
0.50	2.197	1.122	3.874	4.096	6.142	14.577	9.196	38.971
0.40	2.487	1.454	4.269	5.061	6.721	19.955	10.094	53.113
0.30	2.891	2.072	4.788	8.349	7.506	29.573	11.322	78.239
0.20	3.486	3.497	5.535	14.418	8.682	50.355	13.176	132.199
0.10	4.490	8.563	6.854	34.759	10.864	118.450	—	—
0.04	5.760	25.961	8.672	101.230	—	—	—	—
0.01	7.601	119.389	11.549	450.424	—	—	—	—

Table 4. $H_1(\bar{\eta}) = \max_{\eta} H_1(\eta)$.

m	2.0		3.0		4.0	
Pr	$\bar{\eta}$	$H_1(\bar{\eta})$	$\bar{\eta}$	$H_1(\bar{\eta})$	$\bar{\eta}$	$H_1(\bar{\eta})$
5.00	3.894	2.381	6.617	7.091	9.927	16.149
4.00	4.457	3.400	7.588	10.347	11.393	23.694
3.00	5.256	5.411	9.003	16.757	13.534	38.526
2.50	5.850	7.267	10.002	22.648	15.044	52.135
2.00	6.617	10.401	11.337	32.561	17.063	75.007
1.80	7.004	12.303	12.011	38.557	18.084	88.828
1.60	7.456	14.823	12.800	46.484	19.276	107.093
1.40	7.993	18.272	13.737	57.313	20.695	132.029
1.20	8.646	23.193	14.879	72.730	22.423	167.511
1.00	9.465	30.614	16.311	95.921	24.591	220.856
0.90	9.961	35.857	17.179	112.277	25.906	258.463
0.80	10.536	42.697	18.186	133.592	27.429	307.461
0.70	11.212	51.901	19.371	162.239	—	—
0.60	12.027	64.783	20.799	202.287	—	—
0.50	13.035	83.782	22.568	261.284	—	—
0.40	14.335	113.935	24.850	354.819	—	—
0.30	16.114	167.402	—	—	—	—

Table 4 (cont.). $H_1(\bar{\eta}) = \max_{\eta} H_1(\eta)$.

m	0.0		0.5		1.0		1.5	
Pr	$\bar{\eta}$	$H_2(\bar{\eta})$	$\bar{\eta}$	$H_2(\bar{\eta})$	$\bar{\eta}$	$H_2(\bar{\eta})$	$\bar{\eta}$	$H_2(\bar{\eta})$
5.00	1.113	0.053	1.452	0.112	1.824	0.217	2.099	0.355
4.00	1.139	0.064	1.494	0.137	1.877	0.276	2.150	0.458
3.00	1.177	0.080	1.555	0.180	1.948	0.378	2.211	0.640
2.50	1.204	0.093	1.596	0.216	1.992	0.464	2.248	0.791
2.00	1.239	0.111	1.649	0.270	2.046	0.598	2.288	1.024
1.80	1.256	0.122	1.675	0.301	2.070	0.674	2.305	1.156
1.60	1.277	0.134	1.704	0.340	2.096	0.772	2.324	1.323
1.40	1.301	0.151	1.737	0.391	2.124	0.899	2.343	1.541
1.20	1.330	0.172	1.776	0.462	2.155	1.073	2.363	1.834
1.00	1.366	0.203	1.821	0.563	2.188	1.322	2.384	2.249
0.90	1.388	0.224	1.846	0.632	2.206	1.490	2.395	2.527
0.80	1.413	0.249	1.874	0.719	2.224	1.702	2.406	2.874
0.70	1.442	0.283	1.904	0.834	2.243	1.978	2.417	3.330
0.60	1.476	0.328	1.937	0.990	2.263	2.350	2.429	3.935
0.50	1.516	0.393	1.973	1.213	2.284	2.876	2.441	4.786
0.40	1.565	0.492	2.013	1.554	2.306	3.671	2.453	6.068
0.30	1.625	0.663	2.056	2.135	2.329	5.007	2.465	8.210
0.20	1.701	1.015	2.104	3.318	2.352	7.699	2.478	12.506
0.10	1.797	2.113	2.156	6.930	2.377	15.815	—	—
0.04	1.867	5.490	2.190	17.858	—	—	—	—
0.01	1.907	22.514	2.208	72.626	—	—	—	—

Table 5. $H_2(\bar{\eta}) = \min_{\eta} H_2(\eta)$.

m	2.0		3.0		4.0	
Pr	$\bar{\eta}$	$H_2(\bar{\eta})$	$\bar{\eta}$	$H_2(\bar{\eta})$	$\bar{\eta}$	$H_2(\bar{\eta})$
5.00	2.267	0.495	2.412	0.723	2.441	0.870
4.00	2.309	0.643	2.438	0.932	2.458	1.112
3.00	2.357	0.898	2.466	1.285	2.476	1.517
2.50	2.384	1.107	2.482	1.571	2.485	1.843
2.00	2.413	1.427	2.497	2.002	2.495	2.333
1.80	2.425	1.606	2.504	2.243	2.499	2.606
1.60	2.437	1.832	2.510	2.544	2.502	2.948
1.40	2.450	2.125	2.517	2.933	2.506	3.387
1.20	2.464	2.517	2.524	3.452	2.510	3.973
1.00	2.477	3.069	2.530	4.179	2.514	4.793
0.90	2.484	3.439	2.534	4.665	2.516	5.341
0.80	2.491	3.90.	2.537	5.272	2.518	6.025
0.70	2.498	4.499	2.541	6.549	2.520	6.906
0.60	2.506	5.296	2.544	7.096	—	—
0.50	2.513	6.414	2.548	8.556	—	—
0.40	2.521	8.094	2.551	10.748	—	—
0.30	2.528	10.896	—	—	—	—

Table 5 (cont.). $H_2(\bar{\eta}) = \min_{\eta} H_2(\eta)$.

5. REFERENCES.

[1] N. Rott and W. S. Lewellen, 'Boundary layers due to the combined effects of rotation and translation', *Phys. Fluids*, **16**, 1867–1873 (1961).

[2] C. C. Lin, 'Note on a class of exact solutions in magnetohydrodynamics', *Arch. Rat. Mech. Anal.*, **1**, 1–11 (1957).

[3] S. S. Chawla and A. R. Verma, 'Free convection from a disk rotating in a vertical plane', *J. Fluid Mech.*, **126**, 307–313 (1983).

[4] E. M. Sparrow and R. D. Cess, 'MHD flow and heat transfer about a rotating disk', *ASME J. App. Mech.*, **29**, 181–187 (1962).

[5] T. von Karman, 'Uber laminare und turbulente reibung', *ZAMM*, **1**, 233–252 (1921).

[6] W. G. Cochran, 'The flow due to a rotating disk', *Proc. Camb. Phil. Soc.*, **30**, 365–375 (1934).

[7] H. E. Fettis, *Proc. Midwest Conf. Fluid Mech.*, Purdue, 93–104 (1955).

[8] E. R. Benton, 'On the flow due to a rotating disk', *J. Fluid Mech.*, **24**, 781–799 (1966).

[9] C. deBoor, 'A practical guide to splines', Springer-Verlag, New York, (1978).

[10] L. T. Watson and L. R. Scott, 'Solving Galerkin approximations to nonlinear two-point boundary value problems by a globally convergent homotopy method', *SIAM J. Sci. Stat. Comput.*, **8**, 768–789 (1987).

[11] J. J. Moré, B. S. Garbow and K. E. Hillstrom, 'User guide for MINPACK-1', ANL-80-74, Argonne National Laboratory, (1980).

[12] L. T. Watson, S. C. Billups and A. P. Morgan, 'Hompack: A suite of codes for globally convergent homotopy algorithms', *ACM Trans. Math. Software*, **13**, 281–310 (1987).

[13] L. T. Watson, 'Engineering applications of the Chow-Yorke algorithm', *Appl. Math. Comput.*, **9**, 111–133 (1981).

[14] L. T. Watson, 'Numerical study of porous channel flow in a rotating system by a homotopy method', *J. Comput. Appl. Math.*, **7**, 21–26 (1981).

[15] L. T. Watson, 'A globally convergent algorithm for computing fixed points of C^2 maps', *Appl. Math. Comput.*, **5**, 297–311 (1979).

[16] S. K. Kumar, W. I. Thacker and L. T. Watson, 'Magnetohydrodynamic flow and heat transfer about a rotating disk with suction and injection at the disk surface', *Computers & Fluids*, **16**, 183–193 (1988).

[17] S. K. Kumar, W. I. Thacker and L. T. Watson, 'Magnetohydrodynamic flow past a porous rotating disk in a circular magnetic field', *Int. J. Numer. Methods Fluids*, to appear.

[18] S. K. Kumar, W. I. Thacker and L. T. Watson, 'Rotating magnetohydrodynamic flow in a circular magnetic field', Tech. Rep. 321, Dept. of Computer Science, Winthrop College, Rock Hill, S.C. (1987).

[19] S. K. Kumar, W. I. Thacker and L. T. Watson, 'Magnetohydrodynamic flow between a solid rotating disk and a porous stationary disk', Tech. Rep. 314, Dept. of Computer Science, Winthrop College, Rock Hill, S.C. (1987).

CAPTIONS.

Figure 1. a) Effect of m on H_1. Pr=1.0, m=1.5, 1.0, .5, 0.0 (top to bottom). b) Effect of m on H_2. a) Pr=1.0, m=4.0, 3.0, 2.0, 1.5, 1.0, .5, 0.0 (top to bottom).

Figure 2. a) Effect of Pr on H_1. m = 1.0, Pr=.2, .3, .4, .6, 1.0, 2.0 (top to bottom). b) Effect of Pr on H_2. m = 1.0, Pr=.2, .3, .4, .6, 1.0, 2.0 (top to bottom).

Figure 1a

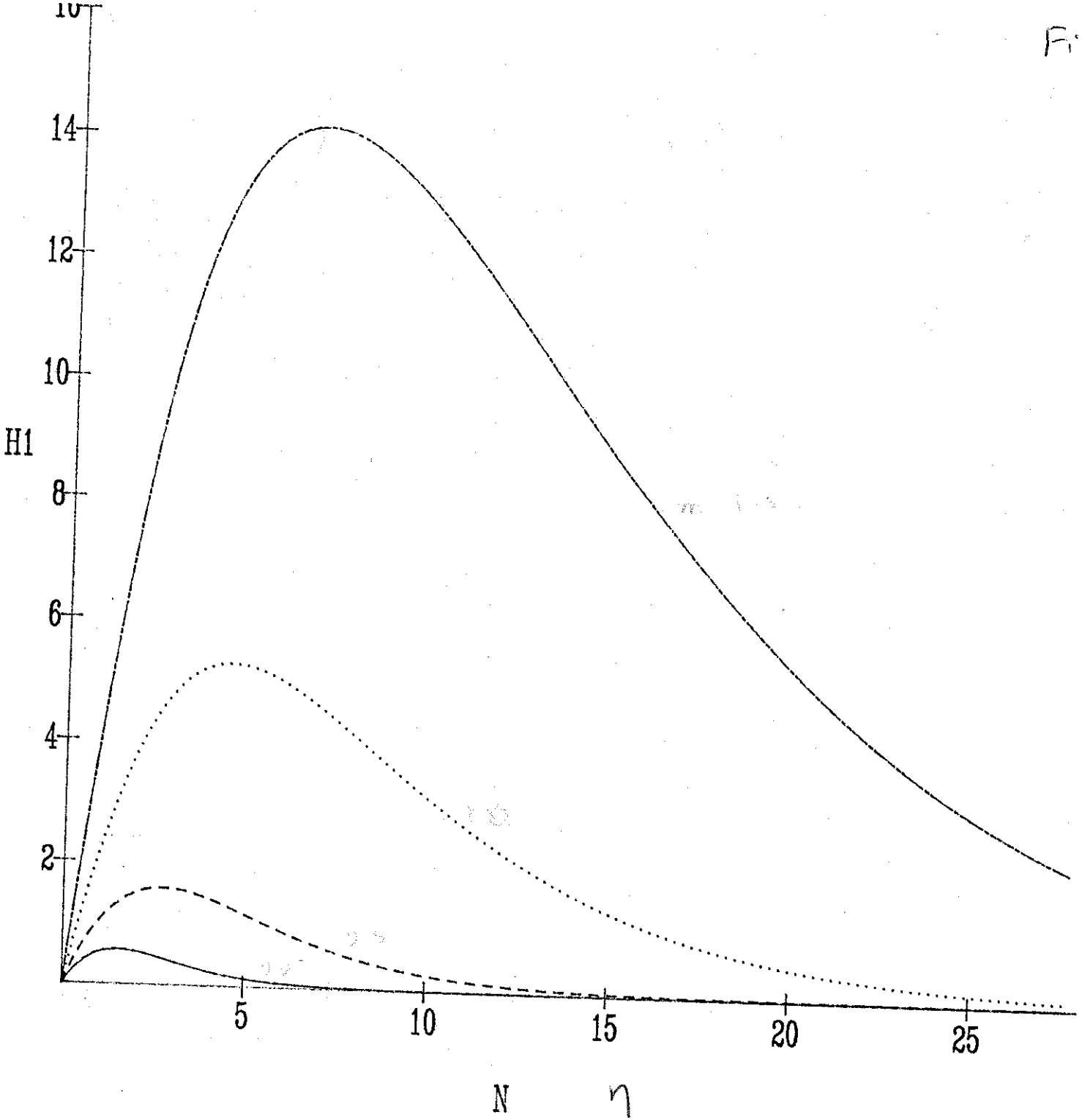

Figure 16

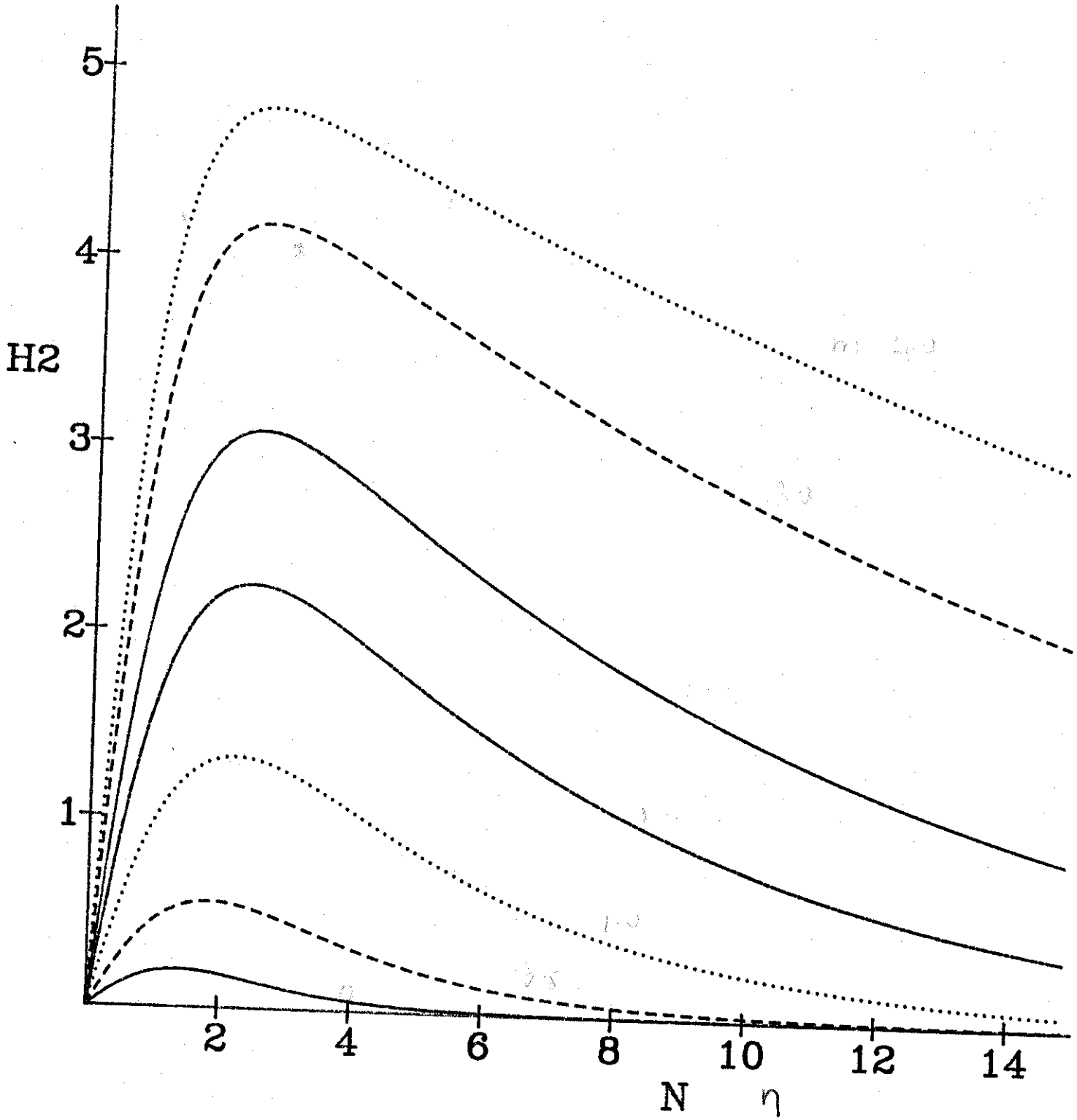

Figure 2a

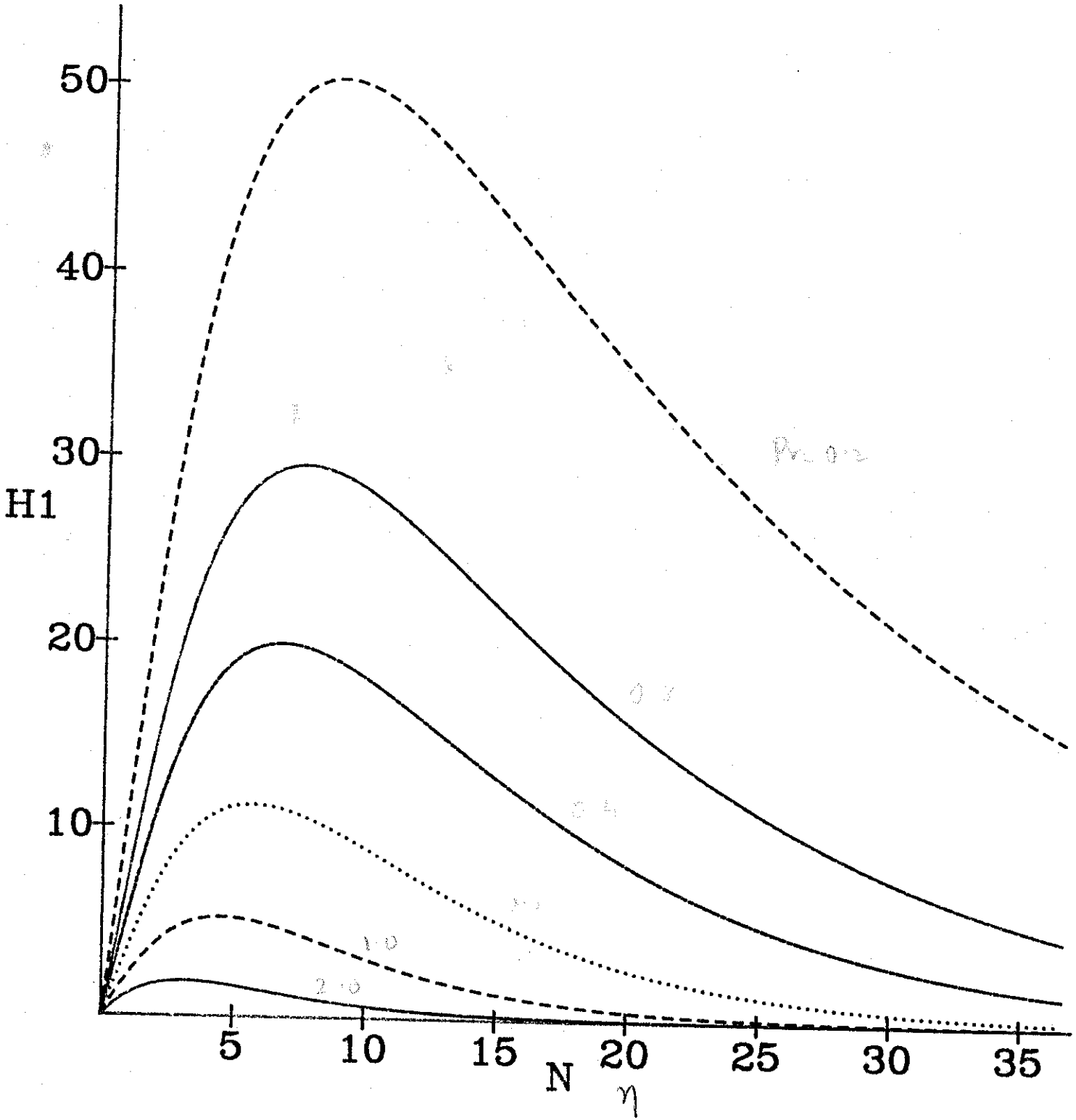

Figure 2b